JOURNAL OF MATERIALS SCIENCE 32 (1997) 469–474

Low pressure injection moulding of SiC platelet reinforced reaction bonded silicon nitride

T. KOSMAC
''Josef Stefan'' Institute, University of Ljubljana, Ljubljana, Slovenia
R. JANSSEN
Advanced Ceramics Group, Technische Universität Hamburg-Harburg, Germany

Reaction-bonded Si_3N_4 toughened by oriented SiC platelets was fabricated via low pressure injection moulding (LPIM). Initially, the rheology of ceramic suspensions was optimized with respect to solid content, SiC platelet loading, particle surface properties and binder composition. Surface active additives were used to modify the particle–polymeric binder interphase in order to prevent particle reagglomeration, to reduce the viscosity and/or to increase the solid content. The relationship between LPIM processing variables and platelet orientation in injection moulded reaction bonded silicon nitride ceramics was studied and the resultant mechanical properties were compared to composites containing randomly dispersed platelets.

1. Introduction

There has been considerable success in reinforcing structural ceramic materials by anisometric particles of various shapes and aspect ratios [1–3]. It has been shown that a significant increase in fracture resistance can be achieved if the reinforcing particles are embedded within the matrix in such a way that, once the material is overloaded and the crack starts propagating, debonding, pull-out and crack bridging occur [4]. Generally, the above mentioned toughening mechanisms are favoured, if the particle/matrix interphase is relatively weak (as compared to the matrix) and are most efficient with particles aligned parallel to the main external stress direction [5]. Another important aspect of particle alignment in ceramic matrix composites is related to the critical defect size for crack initiation, especially if particles are large compared to the matrix grain size (which is usually the case at least for one particle dimension), and if they are not appropriately oriented. Once the particle/matrix interphase becomes the strength-controlling defect, a substantial strength degradation can occur inspite of the somewhat increased fracture toughness, which may represent a serious limitation for particle reinforcement. Although there are ways to achieve perfect particle alignment, they are scarcely used in practice due to poor manufacturing feasibility and the related high production costs. Therefore, for most structural applications, a random distribution of smaller particles or, preferably, a partial alignment accessible to several ceramic forming techniques, are favoured. In particular, it has been demonstrated that noticeable particle alignment can be achieved by wet or plastic forming techniques such as tape casting, slip casting, pressure filtration and powder injection moulding (PIM) [6–11]. The latter also allows complex shaping which, together with its mass production capability, makes this the most promising technique for the fabrication of smaller, complex shaped structural parts.

Furthermore, for those applications, where near-net-shaping and low production costs are of prime importance rather than superior physical and/or chemical properties, reaction forming represents an attractive alternative to conventional ceramic processing procedures. Reaction bonded ceramics (RBC) are fabricated most frequently from metallic powder compacts, which are converted to ceramics by *in situ* reactions or by reactions with liquid or gaseous phases. This process has been most intensively studied in nonoxide systems, such as reaction bonded silicon nitride (RBSN) [12] and carbide (RBSC) [13], and is now also successfully applied in oxide systems, such as reaction bonded alumina (RBAO) and mullite (RBM) [14]. Moderate raw material costs, low processing temperatures and, particularly, low-to-zero-shrinkage capability, arising from volume expansion associated with the metal/ceramic conversion, are the major factors contributing to the reduced production costs of RBC. Furthermore, if a zero- shrinkage material can be preformed by a suitable near net-shaping technique, substantial savings on final machining can also be envisaged. Therefore, we focus in the present study on RBSN composites formed by powder injection moulding following the low-pressure configuration [15]. The potential of particle alignment is studied using SiC platelets due to the compatibility with the Si_3N_4 matrix and their benefits with respect to health hazard, powder processing feasibility and price, e.g., compared with respective whiskers [5, 16].

0022–2461

2. Experimental procedures

As received starting ceramic constituents i.e, Si powder (Kema Nord, Grade 4) and SiC platelets (C-Axis, SC-29), were first oven dried overnight at 150 °C to reduce the moisture content to below 0.2 wt %. The powder/wax batches were prepared using a double planetary mixer equipped with a heating coil. Paraffin-wax and surfactants were melted and, the silicon powder or premixed Si/SiC platelets mixture was added incrementally at 10 min intervals thus allowing each portion to mix thoroughly. After all the material had been added, the entire batch was mixed for 1 h and extruded twice through a single stand die to preserve homogeneity. The viscosity of the blends was measured as a function of shear rate using a standard (Haake VT 500) rotational viscometer. The low pressure injection moulding (LPIM) machine (laboratory constructed) allowed small (≈ 50 g) batches to be de-aired and moulded at pressures up to 7×10^5 Pa and at temperatures up to 90 °C. A metallic mould having the geometry of a 4-point bending test bar $4 \times 4 \times 40$ mm^3 was used for evaluating the injection moulding ability of the blends, as well as the platelet orientation in moulded specimens. The latter was determined at different sections of the molded parts using an optical image analysis system. A core ejector pin system located at the bottom of the bar was used for mould filling. Special care was devoted to thermal debinding: the specimens were embedded in high specific surface area alumina powder (GX Grade, Martinswerk, Germany, Brunauer–Emmett–Teller (BET) surface area > 130 m^2) and slowly heated (20 °C per h) up to 800 °C in flowing nitrogen. Subsequently, some of the specimens were cold isostatically pressed (CIP). For comparison, samples containing the same amount of randomly dispersed platelets were prepared by cold isostatic pressing of uniaxially preformed compacts, using 1 wt % polyvinyl-butyral and 0.5 wt % polyethylene as binder and plasticizer, respectively.

Nitridation was performed in one batch in a cold wall vacuum furnace using a nitrogen demand control system [16]. The maximum temperature during reaction bonding was set to 1450 °C. Pure nitrogen was used as the reaction atmosphere. The per cent of nitridation was examined using sample weight gain and X-ray diffraction. The bulk densities were determined through measurement of each individual bar's dimensions and weight. The pore size was analysed by Hg intrusion. The fracture strength was measured in 4-point-bending according to German standard DIN 51110 but with rectangular bars of reduced length and loading spans of 10 and 20 mm. The tensile side was ground and polished to a 3 μm surface finish to remove surface flaws and the edges were bevelled. The fracture toughness was determined by indentation strength in bending.

3. Results and discussion

For low pressure injection moulding, paraffin wax is usually used as the main binder constituent due to its small molecular size, thermoplastic character and low melting temperature. Beeswax, stearic acid and oleic acid are commonly added to improve the compatibility between powder and binder, and to diminish problems during debinding.

In the case of silicon powder–paraffin blends, the above mentioned additives proved to be effective, however (either separately or in combination) they failed to enable more than 55 vol % of solids loading in the feedstock at an acceptable viscosity for LPIM ($\eta < 30$ Pas at shear rates $D < 10\ s^{-1}$). Although at this solids loading the dimensional stability of moulded parts on debinding is rather high (i.e., linear shrinkage during binder removal is in the range 1–2%) the resultant relative green density ($\approx 55\%$ theoretical density (T.D.)) lies far below the values obtained by cold isostatic pressing of granulated and uniaxially pre-pressed samples (typically 60–65% T.D.). Therefore, octadecyltrimethoxy silane, which has been successfully used as a surface active agent in HPIM polymer/ceramic powder feedstocks [18], was added to reduce the viscosity of the feedstock to such an extent that the solids loading could be increased to 60 vol % and higher. Theoretically, 0.25 wt % of silane molecular weight ($M = 374$ g mol^{-1}, calculated cross section of polar head $A = 0.546$ nm^2) is needed to cover all the surface of the silicone powder (BET ~ 2 m^2 g^{-1}), provided all the silane molecules are adsorbed onto the powder surface. In practice, the addition of 0.5–1.0 wt % of silane was sufficient to decrease the viscosity of the feedstock, e.g., to increase the solids loading to 60 vol % and higher. No further improvement has been reached using higher additions of silane. The flow behaviour of the paraffin-wax/silane blend containing 60 vol % Si-powder is represented in Fig. 1 and it shows at 70, 80 and 90 °C a pronounced pseudoplasticity, which is a commonly observed feature of concentrated aqueous and nonaqueous ceramic suspensions. The temperature dependence of the flow curves enables additional adjustment of the feedstock viscosity by raising or lowering the temperature before injection moulding in the normal manner.

By replacing a part (28 wt %) of the Si powder with SiC platelets, the apparent viscosity of the suspension, as well as its pseudoplasticity and temperature

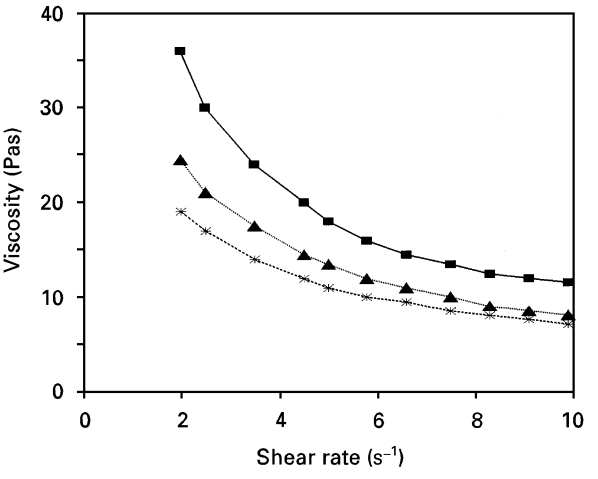

Figure 1 Flow behaviour of Si powder/paraffin wax suspension containing silane coupling agent (1.0 wt % with respect to the 60 vol % solids loading) at (■) 70 °C, (▲) 80 °C and (∗) 90 °C.

dependence are substantially reduced, as is shown in Fig. 2. Due to the interaction between large anisometric particles one would expect that an increased torque will be required for platelet sliding and their alignment in the suspension, which was observed in fibre or whisker containing feedstocks [19]. On the other hand, it is known that the viscosity of a suspension can be decreased by increasing the packing ability of the powder(s) i.e., by introducing a coarse particle fraction into the blend. In the case of $Si/SiC_{pl.}$ system, simplified calculations of packing densities using the model of Onoda (20) predicts an increase in density of about 10% by the addition of 28 wt % large SiC particles. However, the anisometric geometry of the platelets, disregarded in the model, has to be considered as a counteracting effect in the packing behaviour of the powder mixture. It has been demonstrated that the blend of coarse and fine spherical particles will pack better than the mixture of coarse fibres and fine spherical particles, although even in the latter case an increase in packing density can be expected [21]. As is shown in Table 1, the relative density of the loose Si/SiC_{pl} mixture is somewhat lower than that of loose Si powder. If, however, these loose powders were vibrated or cold isostatically pressed, the resultant relative densities of the Si/SiC_{pl} mixtures were higher than the corresponding relative tape and green density of the Si powder alone. A similar observation, namely an increasing relative green density with increasing SiC platelet concentration, was also made by Chou and Green (8) and Selcuk *et al.* [9] on wet formed (slip cast, tape cast) $alumina/SiC_{pl.}$ and $YTZP/SiC_{pl.}$ respectively. It seems therefore that the lower viscosity of the Si/SiC_{pl}–paraffin wax feedstock mainly results from the increased packing density and, to a certain extent, from the reduced specific surface area of the powder mixture to be covered by the liquid vehicle. Less pronounced pseudoplasticity and almost negligible temperature dependence in the temperature range of practical interest (e.g., 70–90 °C) can be primarily regarded as an effect accompanying the considerably reduced apparent viscosity of the suspension, although additional effects, such as platelet alignment and an altered thermal conductivity of the platelet-containing suspension should not be completely disregarded.

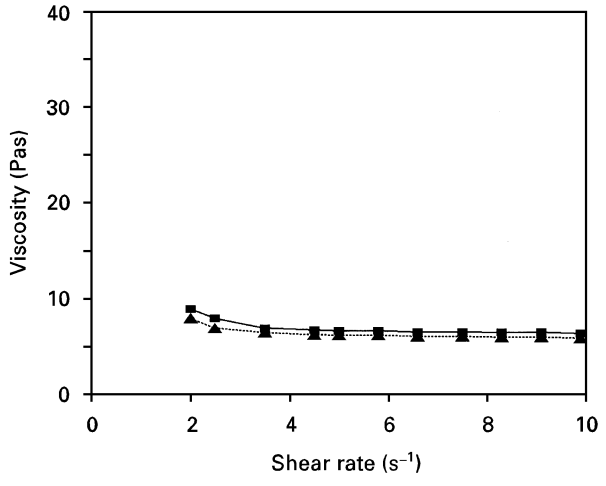

Figure 2 Flow behaviour of $Si/SiC_{pl.}$/paraffin wax suspension containing silane coupling agent (1.0 wt % with respect to the 60% solids loading) at (■) 70 °C and (▲) 90 °C.

TABLE I Relative densities of loose powder (fill density), vibrated powder (tape density) and cold isostatically compacted (640 MPa) powder (green density) for Si and Si/SiC platelet (28 wt %) mixture

Powder	Fill density (%)	Tape density (%)	Green density (%)
Si	27.5	31.0	64.4
Si/SiC_{pl}	26.5	33.5	66.6

The favourable flow characteristics of SiC platelet-containing suspensions and indications of their alignment during viscosity measurement also raised expectations regarding platelet alignment during LPIM which has already been observed in extruded or high pressure injection moulded (HPIM) Si_3N_4/SiC_{pl}-composites [11]. Marshall [22] has reported that a contraction in a flow channel during injection moulding results in the orientation of anisometric particles parallel to the flow direction, whereas expanding flow favours alignment perpendicular to the flow direction. For our experimental work a contracting flow was chosen to fill the mould cavity in a normal filling mode and therefore an alignment of platelets along the flow direction was expected. In fact, the platelets tend to be circumferentially oriented with their *c*-axis (i.e., normal to the basal plane) perpendicular to the flow direction (Fig. 3), except at the very end of the moulded specimens where the feedstock front reached the top of the mould and changed its direction to fill the corners. Thus, only about 30% of the platelets were aligned with their basal plane parallel to the mould filling direction in the polished cross-section just below the top of the moulded specimens. For the rest of the specimens the fraction of platelets having their basal plane parallel to the mould filling direction ranged from 80–90%, whereas the amount of platelets having their basal plane parallel to the surface of rectangular bars along the flow direction was found to be considerably lower and ranged from 45–60% (Fig. 4). It should be noted that the fraction of aligned platelets gradually increased from the gate at the bottom toward the top of the specimens, the tendency being more pronounced at lower moulding pressures. The platelet orientation with respect to the flow direction is thus mainly influenced by the geometric factors determining the flow path and mould filling mode and only to a minor extent by processing variables such as solids loading, slip viscosity and moulding conditions.

On the other hand, variations in feedstock viscosity and moulding pressure introduce considerable changes in the circumferential texture of the aligned platelets. With decreasing slip viscosity and increasing moulding pressure the laminar flow becomes more turbulent, resulting in an "eddy" texture of the platelets although most of them still preserve their *c*-axis oriented perpendicular to the mould filling direction.

The solids loading in the original LPIM feedstock has a profound influence on the fractional density,

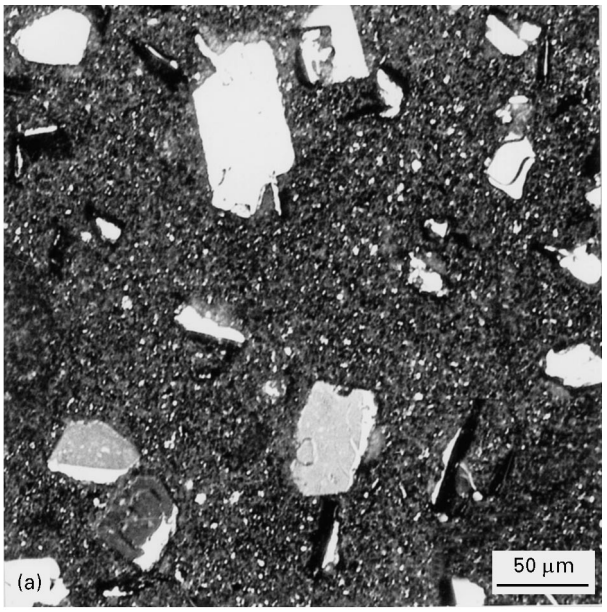

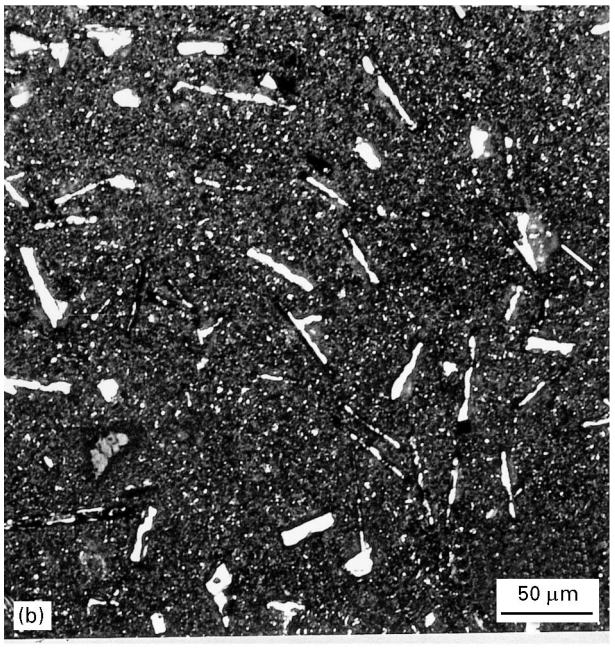

Figure 3 Optical micrographs of injection molded $Si/SiC_{pl.}$ green bodies taken from (a) planes parallel (▲) and (b) perpendicular to the mold filling direction.

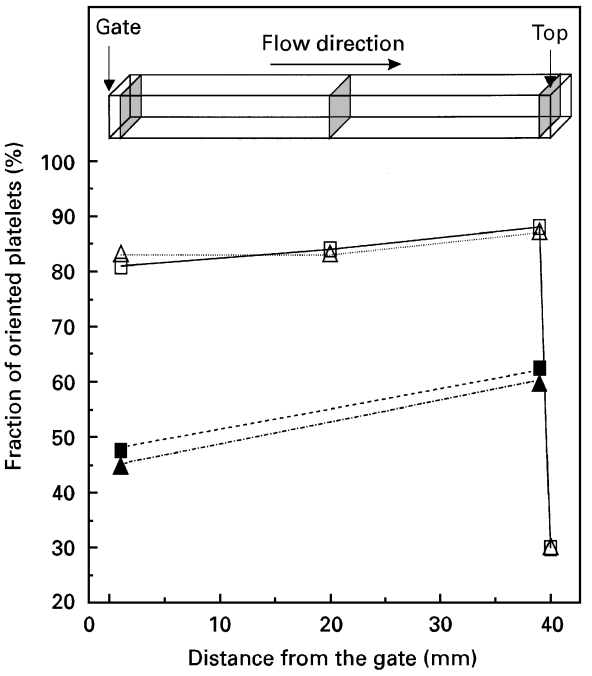

Figure 4 Variation in platelet orientation along the rectangular bars, injection molded at (□) 5 and (△) 7×10^5 Pa. of molding pressure, respectively. Open symbols: fraction of platelets having their *c*-axis perpendicular to the flow direction; filled symbols: fraction of platelets having their basal plane parallel to the surface.

TABLE II Influence of solids loading and post CIP-ing pressure on the fractional density and corresponding average linear shrinkage of injection moulded and post CIP-ed monolithic Si green bodies

Solids loading	After debinding		Debinded + CIP-ed			
			500 MPa		620 MPa	
(vol %)	ρ_{green} (%)	$\Delta l/l_{0_1}$ (%)	ρ_{green} (%)	$\Delta l/l_{0_2}$ (%)	ρ_{green} (%)	$\Delta l/l_{0_2}$ (%)
49	48.5	5.1	66.0	9.7	68.0	10.6
51	50.5	3.2	66.0	8.5	68.0	9.4
57	58.1	≈1	67.0	4.6	68.5	5.3
61	62.6	<1	69.0	3.2	70.0	3.2
UP + CIP (at 500 MPa)	–	–	64.4	–	–	–

ρ_{green} is green density
$\Delta l/l_0$ is shrinkage; l_{0_1} corresponds to the moulded sample, l_{0_2} to the debinded specimen

average size of remnant pores and shrinkage on debinding, although the pore size distribution in debinded samples was found to be rather uniform regardless of the solid loading in the LPIM blend. As shown in Table II, debinding of specimens containing lower solid loadings is accompanied by a noticeable linear size reduction (5.1% for 49 vol % solid loading), whereas specimens containing high solid loading showed almost complete dimensional stability on debinding. Subsequent cold isostatic pressing proved to be capable of eliminating a considerable amount of porosity, indicating a remarkable particle rearrangement. It is worth mentioning that the pre-forming technique prior to cold isostatic pressing played an important role in the CIP-ing ability of the preform. Thus, by CIP-ing injection moulded (IM + CIP) specimens, fractional densities were achieved superior to those obtained from dry pre-formed (UP + CIP) samples.

As expected, all the samples were nitrided near to completion (< 2% of unreacted silicon), regardless of the ceramic forming technique and resulting green density (Table III). However, in injection moulded samples the α and β-Si_3N_4 polytypes are almost equally represented, whereas in dry pressed samples α-Si_3N_4 is predominantly formed. There are also noticeable differences in the fractional weight gain accompanying the conversion of silicon to Si_3N_4. Since the amount of unreacted silicon falls within in a narrow range of 1% for all the specimens, the fractional weight gain mainly reflects the amount of silicon evaporated during the nitridation process. Thus, a fractional weight gain of 93.2% in CIP specimens corresponds to a 2.2% loss of initial silicon (which is in the

TABLE III Characteristics of monolithic RBSN samples, formed by injection molding (IM), IM + CIP-ing and uniaxial prepressing UP + CIP-ing

Forming	Green density (%.T.D.)	Si_3N_4[(b)] (%)	$\frac{\alpha}{\alpha \oplus \beta}$[(a)]	ΔWG[(c)]	Si_V[(d)] %
IM	62.6	98.3	0.55	0.866	6.2
IM + CIP[(a)]	69.0	98.9	0.51	0.790	11.9
UP + CIP[(a)]	64.4	98.1	0.78	0.932	2.2

[(a)] CIP: at 500 MPa;
[(b)] by X-ray diffraction;
[(c)] fractional weight gain, theoretical = 1;
[(d)] silicon evaporated

TABLE IV Mechanical properties of RBSN based ceramics

Forming	Composition	Density (gcm^{-3})	Bending strength (MPa)	Toughness ($MPam^{1/2}$)
IM	monolithic	2.6	180	2.0
	20 vol % $SiC_{plat.}$	2.7	115	2.7
IM + CIP[(a)]	monolithic	2.7	190	2.0
	20 vol % $SiC_{plat.}$	2.8	140	3.2
UP + CIP[(a)]	monolithic	2.6	240	1.6
	20 vol % $SiC_{plat.}$	2.7	140	2.6

[(a)] CIP: at 500 MPa.

range usually obtained), whereas the value of 86.6% for injection moulded specimens reflects a remarkably higher, i.e. 6.2%, loss of initial silicon by evaporation, although the relative green density of these two sets of samples before nitridation was nearly the same. It is assumed that the ceramic forming technique and, particularly, particle migration during thermal debinding of injection moulded specimens alters the particle packing and therefore the structure of interconnected porosity. As a result, the accessibility of nitrogen gas to the unreacted inner region of the powder compact is reduced and the reaction rate is slowed down. Consequently, the amount of unreacted silicon at a given reaction temperature is higher and so is the evaporation rate. Further size reduction of the open pore channels by post - CIP-ing of debinded moulded compacts thus results in almost 12% loss of initial silicon by evaporation, as calculated by contrasting phase composition and fractional weight gain of only 79%.

A similar trend was observed in SiC-platelet containing composites, although the effect is less pronounced due to enhanced gas permeability in structures containing large particles. It should be noted that tailoring the nitridation cycle, an option not addressed in this analysis, can be used to suppress the silicon loss by evaporation and the formation of β-Si_3N_4, respectively.

The sintered densities and corresponding mechanical properties of monolithic and SiC-platelet (20 vol %) reinforced RBSN ceramics are presented in Table IV. The final density and average bending strength of monolithic samples are both within the range reported for RBSN fabricated by the N_2-demand cycle [16]. The presence of larger pores due to incomplete elimination of trapped air from the feedstock before PIM, more intensive silicon evaporation, as well as the higher amount of β-Si_3N_4 in the reaction product are thought to be the main factors influencing the somewhat lower strength values of injection moulded specimens, in spite of their slightly higher densities. The addition of 20 vol % SiC platelets results in a noticeable reduction in strength in all three sets of samples regardless of the partial platelet alignment accessible to the injection moulding technique, as discussed previously. In an earlier work on platelet reinforced composites [23] it was demonstrated that platelets act as strength controlling defects, thereby lowering the strength of the composite. In the case of randomly dispersed platelets, such as in dry pressed (CIP) composites, the strength controlling defect was found to be mainly determined by the diameter of a single platelet or platelet cluster. It was therefore thought that perfect platelet alignment with the basal plane parallel to the tensile surface would restrict the flaw size to the platelet thickness, which should at least preserve the strength of the monolithic RBSN. Low pressure injection moulding, however, does not have the potential for such a perfect platelet alignment. It is capable of aligning most of the platelets with their *c*-axis perpendicular to the mould filling direction but far less with their basal planes parallel to the tensile surface.

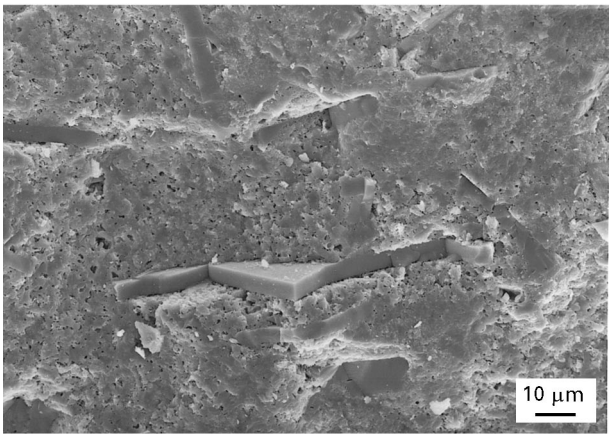

Figure 5 Fracture surface of an injection molded RBSN/$SiC_{pl.}$ composite revealing an almost random orientation of the platelet basal plane with respect to the fracture plane.

This was further confirmed by the scanning electron microscopy (SEM) examination of fractured surfaces (Fig. 5) which revealed an almost random orientation of the platelet's basal planes with respect to the fracture plane, although most of them had their *c*-axis parallel to the fracture plane. Anticipating that those platelets which do not have their basal plane perpendicular to the fracture surface can act as a strength controlling defect, it is obvious that the bending strength of injection moulded samples cannot significantly differ from the strength of CIP-ed specimens.

At the expense of somewhat lower strength though, the fracture toughness of reinforced RBSN is enhanced by the presence of SiC platelets. As is shown in

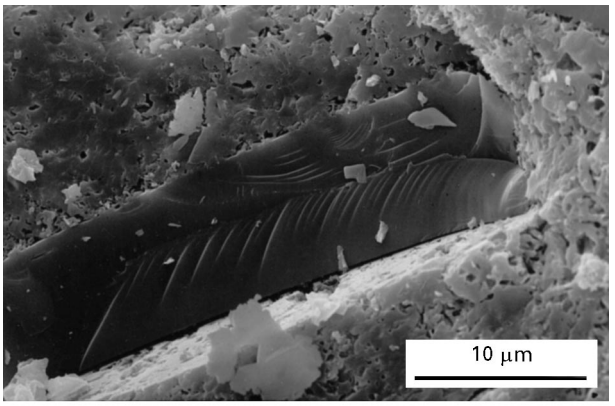

Figure 6 SEM micrograph of a fracture surface of injection molded RBSN/$SiC_{pl.}$ composite showing partial debonding and cleavage of a platelet.

Fig. 6, most frequently the crack propagates by partial debonding and cleavage. Here again, the partial platelet alignment accessible to PIM seems to have only limited influence on the fracture toughness of the composites. Instead, a systematic increase of about 20% in fracture toughness was observed with all the injection moulded specimens, as compared to the corresponding dry CIP-ed samples. With reference to Table III, besides platelet alignment the most evident difference between injection moulded and dry CIP-ed RBSN specimens is a lower $\alpha/(\alpha + \beta)$ Si_3N_4 ratio which also alters the fracture toughness.

4. Conclusions

It has been demonstrated that the addition of silane reduces the viscosity of a paraffin/Si-powder feedstock for low pressure injection moulding such that rather high (60 vol% and higher) solid loading can be achieved. The presence of large, fully dense SiC platelets further reduces the viscosity of the feedstock, mainly due to reduced surface area and increased fractional density of the powder mixture.

Low pressure injection moulding has a potential of aligning most (80–90%) of the platelets with their normals to the basal plane perpendicular to the mould filling direction but far less with their basal planes parallel to the surface of the moulded body. The fraction of oriented platelets gradually increases from the gate toward the top of the moulded part, the tendency being more pronounced at lower moulding pressures. The remaining unaligned platelets still act as strength controlling defects, reducing the strength of the injection moulded composites to values which are typically obtained with composites containing randomly dispersed platelets.

Acknowledgement

The work was performed within the bilateral Slovenian-German Cooperation in Scientific Research and Technological Development. The financial support of the Internationales Büro der KFA Jülich and Slovenian Ministry of Science and Technology is gratefully acknowledged.

References

1. R. W. RICE, *Ceram. Engng Sci. Proc.* **6** (1985) 589.
2. A. G. EVANS and R. M. MCMEEKING, *Acta Metall* **34** (1986) 2435.
3. P. F. BECHER, C. S. HSUEH, P. ANGELINI and T. N. TIEGS, *J. Amer. Ceram. Soc.* **71** (1988) 1050.
4. A. G. EVANS, *ibid* **73** (1990) 187.
5. N. CLAUSSEN, Proceedings of the 11th Riso International Symposium on Metallurgy and Materials Science, edited by J. J. Bentzen, J. B. Bilde-Sorensen, N. Christiansen, A. Housewell and B. Ralph, Riso National Laboratory, Roskilde, Denmark 1990.
6. D. A. WARNER and D. T. SORENSEN, in "Euroceramics II, Vol. 2: Structural Ceramics and Composites", edited by G. Ziegler and H. Hausner, Cologne, DKG, 1993, 1647.
7. M. WU and G. L. MESSING, *J. Amer. Ceram. Soc.* **77** (1994) 2586.
8. Y.-S. CHOU and D. J. GREEN, *ibid* **75** (1992) 3346.
9. A. SELCUK, C. LEACH and R. D. RAWLINGS, *J. Eur. Ceram. Soc.* **15** (1995) 33.
10. T. CLASSEN and N. CLAUSSEN, *ibid* **10** (1992) 263.
11. S. J. STEDMAN, J. R. G. EVANS, R. J. BROOK and M. J. HOFFMANN, *ibid.* **11** (1993) 523.
12. J. MOULSEN, *J. Mater. Sci.* **14** (1979) 1017.
13. N. L. PARR, G. F. MARTIN and R. W. MAY, in Special Ceramics, edited by P. Popper, Heywood, London, 1960.
14. N. CLAUSSEN, R. JANSSEN and D. HOLZ, *J. Ceram. Soc. Jpn.* **108** (1995) 749.
15. J. A. MANGELS, *Amer. Ceram. Soc. Bull.* **73** (1994) 37.
16. R. JANSSEN and N. CLAUSSEN, in: Proceedings First. International Symposium on Science of Engineering Ceramics, edited by S. Kimura and K. Niihara, Ceramic Society of Japan, Tokyo, **1** (1991) 371.
17. J. A. MANGELS, *Ceram. Bull.* **60** (1981) 613.
18. G. ZHANG, M. J. EDINGSINGHE and J. R. G. EVANS, *J. Mater. Sci.* **23** (1988) 2115.
19. D. SACKS, H.-W. LEE and O. E. ROJAS, *J. Amer. Ceram. Soc.* **71** (1988) 370.
20. G. Y. ONODA, in Proceedings of Ceramic Microstructures '76, Boulder, CO, edited by R. M. Fulrath and J. A. Pask, Westview, Boulder, Co. (1976) 163.
21. S. BLACKBURN and H. BÖHM, *J. Mater. Sci.* **29** (1994) 4157.
22. D. F. MARSHALL, *Materials and Design* **8** (1987) 77.
23. R. JANSSEN and K. H. HEUSSNER, *Powder Metall. Int.* **23** (1991) 241.

Received 8 January
and accepted 17 July 1996